PROTEINS
STRUCTURE ■ FUNCTION ■ BIOINFORMATICS

SHORT COMMUNICATION

Solution NMR studies reveal no global flexibility in the catalytic domain of CDC25B

George Lund and Tomasz Cierpicki*

Department of Pathology, University of Michigan, Ann Arbor, Michigan

ABSTRACT

The CDC25B phosphatase is a critical regulator of the cell cycle and has been validated as an important therapeutic target in cancer. Previous studies using molecular dynamics simulations have concluded that the catalytic domain of CDC25B may experience a significant degree of dynamics or be partially disordered in solution, a finding that has a pronounced impact on the structure-based development of CDC25B inhibitors. We have probed the backbone dynamics of the CDC25B catalytic domain in solution using NMR relaxation experiments and found that the core of the protein is relatively rigid and does not experience any large-scale dynamics over a broad range of time scales. Furthermore, based on residual dipolar coupling measurements we have concluded that the conformation in solution is very similar to that observed in the crystal form. Importantly, these findings rationalize the application of the CDC25B crystal structure in structure-based drug development.

Proteins 2014; 82:2889–2895.

Key words: NMR dynamics; CDC25B; model-free analysis; protein dynamics; protein structure; RDC.

INTRODUCTION

The CDC25 dual-specificity phosphatases are key regulators of the cell cycle, and their role in cancer has led to their active targeting of small molecule inhibitor development for over two decades.[1–4] CDC25 phosphatases are critical activators of CDK/cyclin complexes by removing inhibitory phosphorylations on CDK family kinases.[5] As a downstream target of the DNA damage response pathway, the CDC25 phosphatases play an important role in maintaining genomic stability after DNA damage. All three phosphatases, CDC25A, CDC25B, and CDC25C, have been shown to be overexpressed in primary samples from a variety of tumor types, often correlating with a poor patient prognosis.[6,7] Because of its potential as a therapeutic target in cancer, studies on CDC25 family catalytic mechanism and structure are of vital importance. Previous molecular dynamics (MD) simulations combined with bioinformatics analysis have suggested that approximately 20 C-terminal residues of CDC25B are partially unfolded or disordered in solution.[8,9] It has been hypothesized that dynamics of the C-terminus allows for the formation of transient pockets near the active site.[8,9] This finding may directly impact development of CDC25B inhibitors and may present a warning against using the crystal structure of CDC25B for structure-based drug design.[9] Therefore, the need for experimental characterization of the dynamics of CDC25B has been emphasized in the literature.[9]

Additional Supporting Information may be found in the online version of this article.

Grant sponsor: University of Michigan Gastrointestinal (GI) Specialized Programs of Research Excellence (SPORE) Career Development Award; Grant sponsor: NIH; grant number: R01 CA181185.

*Correspondence to: Tomasz Cierpicki, 4510C MSRBI, 1150 W. Medical Center Drive, Ann Arbor, MI 48109-5620. E-mail: tomaszc@umich.edu

Received 17 January 2014; Revised 1 April 2014; Accepted 8 April 2014
Published online 17 April 2014 in Wiley Online Library (wileyonlinelibrary.com).
DOI: 10.1002/prot.24581

In this study, we have characterized the dynamics of the CDC25B catalytic domain using NMR relaxation experiments on various time scales, as well as evaluated the structure of CDC25B in solution using residual dipolar couplings. In contrast to the predictions from MD simulation,[8,9] we found that CDC25B is a relatively rigid protein with a very well-defined structure of the C-terminal helical fragment and the overall conformation in solution is very close to that observed in the crystal structure. Ultimately, our results have important implications for the structure-based design of small molecule inhibitors of CDC25B.

METHODS

Expression and purification of the CDC25B catalytic domain

The CDC25B catalytic domain (372–551) and variants were expressed in *E. coli* BL21 (DE3) with an N-terminal GST tag. The CDC25B cDNA with an N-terminal tobacco etch virus (TEV) protease cleavage site was purchased from Genscript and cloned into a pGST-21a vector with NcoI/XhoI. Cells were grown in either luria broth (LB) or labeled M9 medium. After 16 h induction with 0.5 m*M* isopropyl beta-D-1-thiogalactopyranoside (IPTG) at 18°C, *E. coil* cells were lysed by cell disruption in a buffer containing 50 m*M* Tris (pH 8.0), 150 m*M* NaCl, 1 m*M* TCEP, and 0.5 m*M* phenylmethanesulfonyl fluoride (PMSF). The cell lysate was subjected to centrifugation, after which the soluble fraction was incubated with glutathione resin. The resin was then washed with lysis buffer, and eluted with lysis buffer containing 50 m*M* L-glutathione. The eluate was proteolytically cleaved with TEV protease, followed by S-75 size exclusion chromatography in buffer containing 50 m*M* Tris (pH 8.0), 50 m*M* NaCl, and 1 m*M* TCEP. Pure fractions were pooled and frozen at −80°C.

NMR spectroscopy and assignment of CDC25B catalytic domain

Samples for backbone assignment were made with $^{13}C^{15}N$-labeled CDC25B C473S prepared in a buffer containing 50 m*M* Tris (at either pH 7.0 or 8.0), 50 m*M* NaCl, 1 m*M* TCEP, and 5% D_2O. Spectra were acquired at 30°C on a 600 MHz Bruker Avance III spectrometer equipped with cryoprobe, running Topspin version 2.1. Backbone assignment was done using a series of triple-resonance experiments including HNCACB, CBCA (CO)NH, HNCA, HN(CO)CA, HNCO, HN(CA)CO, and ^{15}N-separated NOESY-HSQC.[10–12] Processing and spectral visualization was performed using NMRPipe[13] and Sparky.[14]

NMR-based relaxation measurements

All relaxation measurements were acquired at 30°C using ^{15}N-labeled CDC25B C473S or the wild-type CDC25B in buffer containing 50 m*M* Tris (pH 7.0), 50 m*M* NaCl, 1 m*M* TCEP, and 5% D_2O. T_1 and T_2 relaxation measurements, as well as the ^1H-^{15}N heteronuclear NOE measurement were obtained using experiments similar to those described by Bax and coworkers.[15] The relaxation delays for the T_1 and T_2 experiments were 10, 30, 70, 150, 330, 750, 1500, 2200 ms, and 17, 34, 51, 68, 85, 102, 136, 170 ms, respectively. ^1H-^{15}N heteronuclear NOE experiments were recorded as interleaved experiments with and without NOE saturation (Supporting Information Fig. S3). Experimental relaxation delays were set at 6 s for T_2 and ^1H-^{15}N heteronuclear NOE measurements, and 4 s for T_1 measurements. T_2 and ^1H-^{15}N heteronuclear NOE experiments were performed in duplicate. T_1 and T_2 values were calculated by fitting relaxation curves in Sparky.[14]

Relaxation dispersion experiments were recorded at 30°C at 600 MHz using a series of Carr–Purcell–Meiboom–Gill (CPMG) pulse trains as reported previously.[16] Two-dimensional spectra were acquired with CPMG field strengths of 25, 50, 75, 150, 300, 750, and 1000 Hz. Peak lists with intensities were used as input into the program NESSY for calculation of $R_{2,\mathrm{eff}}$ and subsequent model fitting.[17]

Model-free analysis

Model-free analysis was performed using the modelfree4 and FASTModelfree programs.[18,19] The PDB structure used was prepared using the pdbinertia program,[20] and the initial estimate for the diffusion tensor ($D_{\mathrm{par/per}}$) was obtained using the r2r1_diffusion program.[21] An axially symmetric diffusion model was used with the following initial parameters: rotational correlation time $\tau_c = 11.4$ μs, diffusion tensor $D_{\mathrm{par/per}} = 1.25$, and rotation angles $\theta = 6.3°$, $\Phi = -220°$, which describe the re-orientation of the molecule to the principal axis system. The protocol for model selection was as described by Mandel *et al.*[22] FASTModelfree was employed to iteratively adjust the global parameters between optimizations of the internal parameters (S^2, τ_c, etc.). The global parameters converged after eight iterations.

Measurement of residual dipolar couplings

Samples for measurement of residual dipolar couplings were made using ^{15}N CDC25B C473S in buffer containing 50 m*M* Tris (pH 7.0), 50 m*M* NaCl, 1 m*M* TCEP, with 5% D_2O and acquired at 30°C. Charged polyacrylamide gels for alignment were prepared as described previously.[23] Samples were prepared for isotropic measurements (gel-free) and two different anisotropic measurements, including a positively charged gel (50+M) and a negatively charged gel (50-S). $^1J_{NH}$ couplings were measured for isotropic and anisotropic samples using the in-phase anti-phase (IPAP) experiment.[24] Residual dipolar couplings

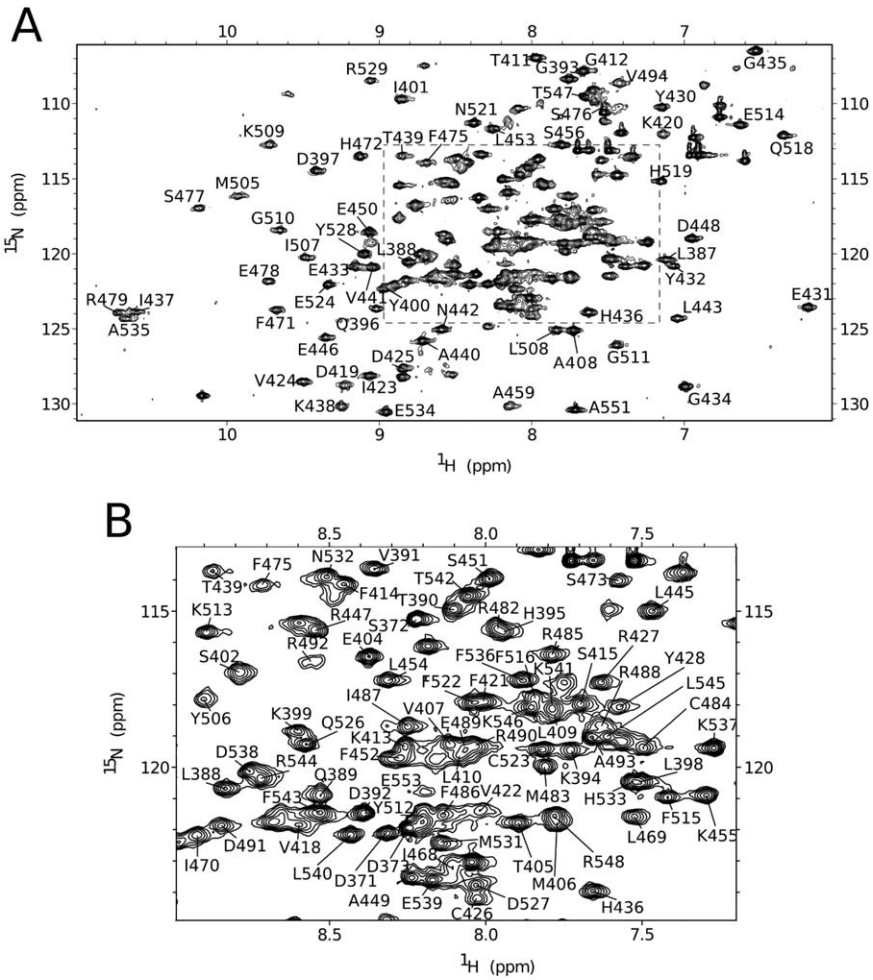

Figure 1

Assignment of CDC25B catalytic domain. **A**: The $^{1}H^{15}N$-HSQC spectrum of the CDC25B catalytic domain is shown with assignments labeled. **B**: Cutout of the overlapped region of the spectrum with assignments.

were calculated by subtracting the $^{1}J_{NH}$ couplings of the isotropic sample from the couplings of the anisotropic sample. Comparison of experimental and predicted residual dipolar coupling (RDC) values was performed with the DC program in NMRPipe,[13] using PDB code 2A2K[25] for the RDC back calculations.

RESULTS

Assignment of the catalytic domain of CDC25B

In order to probe the backbone dynamics of the catalytic domain of CDC25B, we performed the assignment of the CDC25B backbone using triple resonance experiments. Our initial studies revealed that the $^{1}H^{15}N$-HSQC spectrum of CDC25B shows good dispersion of peaks, consistent with well-folded protein. However, we observed that the wild-type protein precipitated out of solution over longer periods of time, leading to reduced quality of NMR spectra. We found that point mutation of the active site cysteine to serine (C473S) substantially improved the long-term protein stability, likely through reducing protein oxidation. We validated that C473S mutation did not affect protein structure and dynamics because both, the backbone chemical shifts (Supporting Information Fig. S1) as well as the backbone ^{15}N T_1, T_2 relaxation times (Supporting Information Fig. S2) for the mutant and the wild-type protein are very similar. Furthermore, it has been shown that the structure of C473S mutant is identical to the wild-type protein.[26] As a result of increased long-term stability, we selected CDC25B C473S variant for characterization using solution NMR.

The ^{1}H-^{15}N HSQC spectrum for the CDC25B C473S shows 155 backbone amides, which constitute 83% of all expected resonances. We have assigned 92% of observed

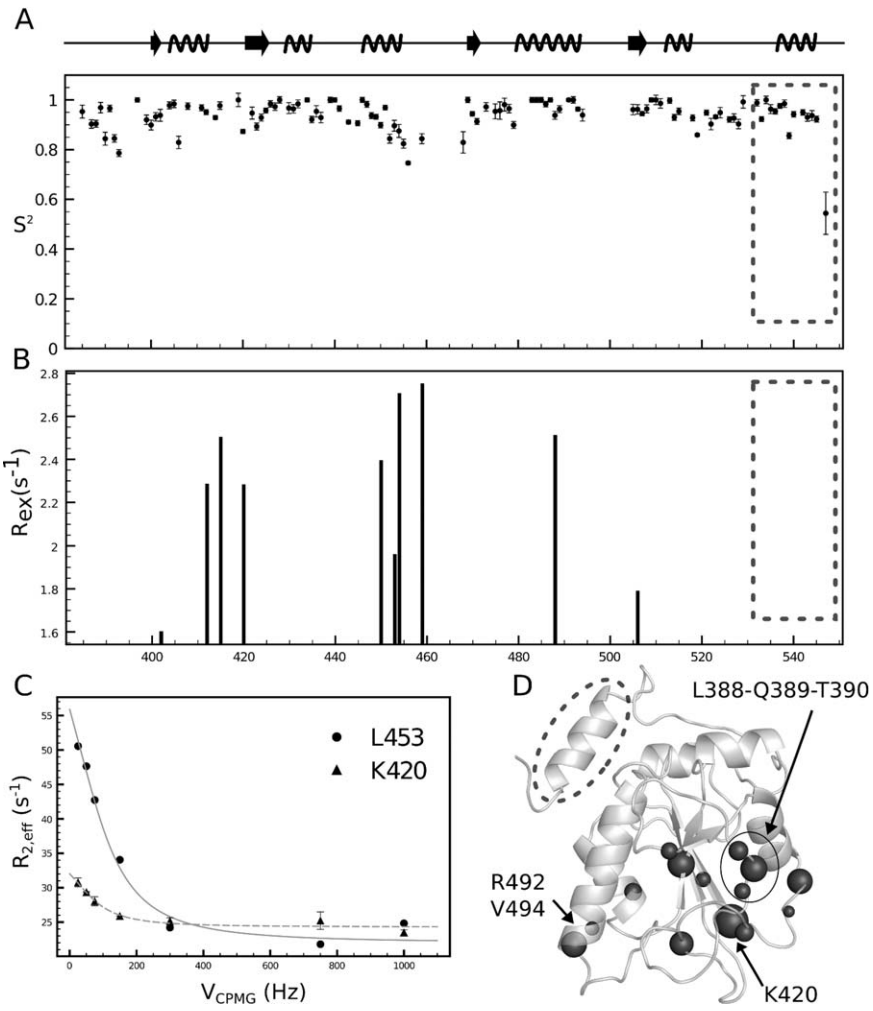

Figure 2

The CDC25B catalytic domain is relatively rigid in solution. **A**: The generalized order parameter (S^2) is shown for the entire sequence as determined by model free analysis, with a box around C-terminal helix denoting the helix previously reported to be dynamic. A schematic of CDC25B secondary structure is shown above. **B**: Additional exchange processes (R_{ex}) on the millisecond timescale, predicted by model free analysis. A box around the C-terminal helix is also shown. **C**: Representative relaxation dispersion plots for K420 and L453 with $R_{2,eff}$ shown as a function of CPMG pulse frequency in Hz. **D**: Crystal structure of CDC25B (PDB: 2A2K) highlighting residues experiencing exchange in the relaxation dispersion experiments. Size of sphere indicates relative magnitude of R_{ex} calculated by relaxation dispersion curve modeling. The C-terminal helix is denoted by the dashed ellipse.

backbone amide resonances by employing triple resonance experiments (Fig. 1). The majority of unobserved amide resonances correspond to N-terminal residues as well as residues located in two loop regions, corresponding to residues 461–467 and 495–504. These regions likely are unobserved due to rapid exchange of the amide protons with water.

The CDC25B catalytic domain is relatively rigid in solution

To explore the backbone dynamics of the CDC25B C473S on the pico-second to nano-second timescale, we measured the R_1 and R_2 relaxation rates as well as the steady state ^{1}H-^{15}N heteronuclear NOE using methodology as previously described.[15] We then used Lipari–Szabo model-free analysis[27] to quantitatively assess fast timescale backbone motions of CDC25B C473S. This analysis yielded an overall averaged order parameter (S^2) of 0.94, indicative of a well ordered backbone with limited internal dynamic motion on the ps–ns timescale [Fig. 2(A)]. Such a relatively high average order parameter may result from a lack of signals for several amides in loop regions, likely due to their fast exchange with water.

The global correlation time determined by the analysis converged to 11.4 μs, consistent with a monomeric

protein. Only a few resonances show order parameters of less than 0.85, and these are exclusively found either at one of the CDC25 termini, or within the internal loop region 461–467. No amides experience an S^2 of less than 0.7, indicating that no section of the assigned protein, including the C-terminal helix, experiences any significant dynamics on this timescale. The model-free analysis also indicates that several residues experience additional exchange processes in the micro-second to milli-second timescale which contribute to the observed relaxation data [Fig. 2(B)]. With the exception of E450 and R488, the remaining residues modeled with R_{ex} contributions appear immediately adjacent to or within loop regions, and all of the residues are farther than 10 Å from the active site. To ensure the dynamics of CDC25B was not altered by the C473S mutation, we measured both R_1 and R_2 relaxation rates for the wild-type protein (Supporting Information Fig. S2). Data obtained from these experiments are highly consistent with the data recorded for the mutant, showing an average deviation of 0.048 s^{-1} and 1.57 s^{-1} for R_1 and R_2, respectively.

To further address the possibility of conformational exchange within the CDC25B C473S mutant catalytic domain on slower, μs–ms time scales, we carried out ^{15}N relaxation dispersion measurements using CPMG experiments.[16] We detected that only a few residues experienced significant exchange in this analysis [Fig. 2(C,D)]. The majority of these residues are within or adjacent to loop regions [Fig. 2(D)]. Several residues form small clusters, for example L388-Q389-T390 or D419-K420-V422 that have relatively similar exchange rates, representing local motion of these groups in the milli-second timescale. Importantly, no motion on μs–ms time scale was observed for any residues within 10 Å of the active site or within the C-terminal helix.

Previous MD simulations indicated that the CDC25B C-terminal residues (amino acids 531–550) are partially unfolded or disordered.[8,9] On the contrary, our experimental studies of the backbone dynamics clearly demonstrates that these residues are well ordered, with an average S^2 of greater than 0.9 for residues in this region. Additionally, a lack of any correlated exchange in this region on the μs–ms timescale indicates that this helix does not undergo any partial unfolding.

Solution structure of CDC25B is very similar as in the crystal form

In order to assess whether the crystal structure of CDC25B correctly reflects the protein conformation in solution or whether the crystal structure is distorted by crystal packing, we measured RDC. RDC measurements accurately reflect the average orientation of a bond vectors relative to a molecular frame of alignment, and thus have been shown to provide reliable data for analysis of structure in solution.[28,29] Specifically, comparing calculated and experimental RDC values is a powerful tool in validating the crystal structure.[28] In order to measure RDCs, we aligned the protein using both positively and negatively charged polyacrylamide gels as described previously.[23] We determined approximately 110 $^1D_{HN}$ RDCs for each alignment (Fig. 3). Comparison between the experimental RDC values and the calculated values from the published CDC25B C473S catalytic domain crystal structure (PDB: 2A2K[25]) yields a very good agreement, with correlation coefficients of 0.96 and 0.97 for the protein in positively and negatively charged alignment media, respectively (Fig. 3). Importantly, RDCs for both the active site residues and the C-terminal helix agree very well with the RDC values predicted from the crystal structure. For example, the correlation coefficients for the RDCs for residues in the C-terminal helix are

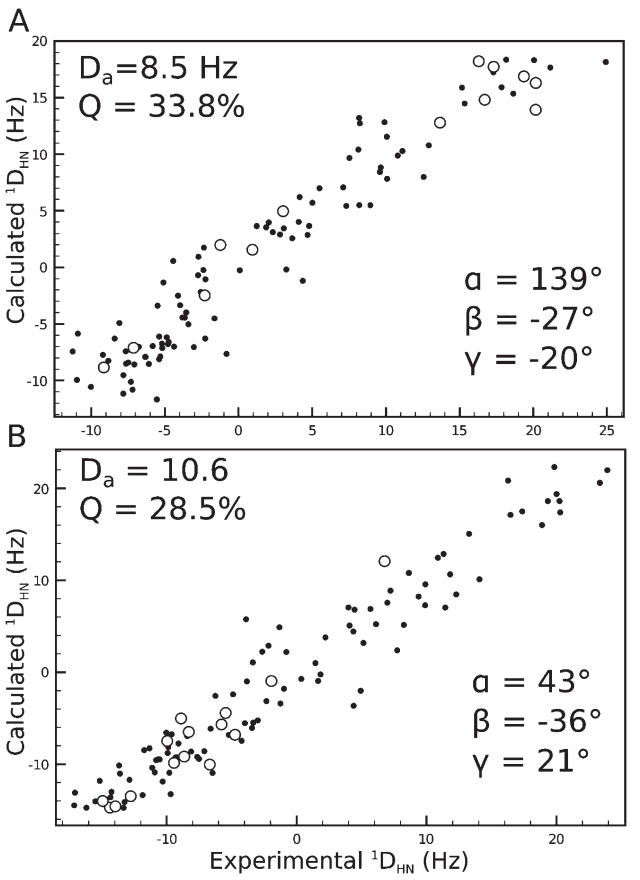

Figure 3

Residual dipolar couplings indicate that CDC25B crystal structure is representative of its structure in solution. **A**, **B**: Correlation of predicted and experimental residual dipolar couplings. Alignment tensor, *Q*-factor, and Euler angles are given. Closed circles represent the CDC25B catalytic domain sequence from 385 to 530, open circles represent the C-terminal helix from 531 to 551. **A**: Correlations for positively charged gel sample (50+M). **B**: Correlations for negatively charged gel sample (50-S).

0.95 and 0.91 in positively and negatively charged gels, respectively. These results from two independent alignments clearly indicate that the structure of CDC25B C473S in solution is very close to the structure determined by X-ray crystallography. To additionally examine the CDC25B C473S conformation in solution, we performed an analysis of the chemical shifts for all assigned resonances using the TALOS+ program,[30] which predicts secondary structure elements from chemical shift data. The resulting secondary elements predicted from this analysis closely match those found in the crystal structure (Supporting Information Fig. S4).

DISCUSSION

In this study, we found that the catalytic domain of CDC25B is relatively rigid in solution, and that the structure in solution is very close to the crystal structure. This finding is in contrast to previous MD studies of this protein; specifically, that the 20 amino acids near the C-terminus that were predicted to be dynamic in solution by MD underwent no such dynamics experimentally.[8,9] Experimental analysis of backbone dynamics on slow timescales shows no conformational exchange in either the C-terminal region or anywhere near the active site, and therefore is highly unlikely to undergo any partial unfolding as previously suggested. Because we observed no backbone dynamics near the active site, it is unlikely that there are any transient or cryptic binding pockets near this site.

In our studies, we focused on experimental characterization of backbone dynamics, and did not explore any potential motion of the side chains. Also, several backbone amides are not observed in our experiments, likely due to fast exchange of the amide protons with water. However, majority of these residues are relatively distant from the active site and the C-terminal helix, which were predicted to be disordered via MD simulations.[9]

Our study has important implications for structure-based small molecule design, since it provides strong evidence that the crystal structure of the CDC25B catalytic domain accurately reflects its conformation in solution. This study further demonstrates a need to experimentally validate findings from MD simulations, particularly in cases where this may directly impact design of small molecule inhibitors.

REFERENCES

1. Boutros R, Lobjois V, Ducommun B. CDC25 Phosphatases in cancer cells: key players? Good targets? Nat Rev Cancer 2007;7:495–507.
2. Kristjánsdóttir K, Rudolph J. Cdc25 Phosphatases and cancer. Chem Biol 2004;11:1043–1051.
3. Lavecchia A, Di Giovanni C, Novellino E. Inhibitors of Cdc25 phosphatases as anticancer agents: a patent review. Expert Opin Ther Pat 2010;20:405–425.
4. Lavecchia A, Di Giovanni C, Novellino E. CDC25 Phosphatase inhibitors: an update. Mini Rev Med Chem 2012;12:62–73.
5. Nilsson I, Hoffmann I. Cell cycle regulation by the Cdc25 phosphatase family. Prog Cell Cycle Res 2000;4:107–114.
6. Takemasa I, Yamamoto H, Sekimoto M, Ohue M, Noura S, Miyake Y, Matsumoto T, Aihara T, Tomita N, Tamaki Y, Sakita I, Kikkawa N, Matsuura N, Shiozaki H, Monden M. Overexpression of CDC25B phosphatase as a novel marker of poor prognosis of human colorectal carcinoma. Cancer Res 2000;60:3043–3050.
7. Ito Y, Yoshida H, Tomoda C, Uruno T, Takamura Y, Miya A, Kobayashi K, Matsuzuka F, Kuma K, Nakamura Y, Kakudo K, Miyauchi A. Expression of cdc25B and cdc25A in medullary thyroid carcinoma: cdc25B expression level predicts a poor prognosis. Cancer Lett 2005;229:291–297.
8. Mamonov AB, Bhatt D, Cashman DJ, Ding Y, Zuckerman DM. General library-based Monte Carlo technique enables equilibrium sampling of semi-atomistic protein models. J Phys Chem B 2009; 113:10891–10904.
9. Arantes GM. Flexibility and inhibitor binding in cdc25 phosphatases. Proteins 2010;78:3017–3032.
10. Schleucher J, Schwendinger M, Sattler M, Schmidt P, Schedletzky O, Glaser SJ, Sørensen OW, Griesinger C. A general enhancement scheme in heteronuclear multidimensional NMR employing pulsed field gradients. J Biomol NMR 1994;4:301–306.
11. Kay LE, Xu GY, Yamazaki T. Enhanced-sensitivity triple-resonance spectroscopy with minimal H_2O saturation. J Magn Reson Ser A 1994;109:129–133.
12. Muhandiram DR, Kay LE. Gradient-enhanced triple-resonance three-dimensional NMR experiments with improved sensitivity. J Magn Reson Ser B 1994;103:203–216.
13. Delaglio F, Grzesiek S, Vuister GW, Zhu G, Pfeifer J, Bax A. NMRPipe: a multidimensional spectral processing system based on UNIX pipes. J Biomol NMR 1995;6:277–293.
14. Goddard TG, Kneller DG. SPARKY 3, University of California, San Francisco.
15. Barbato G, Ikura M, Kay LE, Pastor RW, Bax A. Backbone dynamics of calmodulin studied by 15N relaxation using inverse detected two-dimensional NMR spectroscopy: the central helix is flexible. Biochemistry 1992;31:5269–5278.
16. Tollinger M, Skrynnikov NR, Mulder FA, Forman-Kay JD, Kay LE. Slow dynamics in folded and unfolded states of an SH3 domain. J Am Chem Soc 2001;123:11341–11352.
17. Bieri M, Gooley PR. Automated NMR relaxation dispersion data analysis using NESSY. BMC Bioinformatics 2011;12:421.
18. Palmer AG. Modelfree 4.2. 2006. Accessed July 29, 2013. Available at: http://cpmcnet.columbia.edu/dept/gsas/biochem/labs/palmer/software.html.
19. Cole R, Loria JP. FAST-Modelfree: a program for rapid automated analysis of solution NMR spin-relaxation data. J Biomol NMR 2003:26;203–213.
20. Palmer AG. pdbinertia. Version 4.2, 2006. Accessed July 29, 2013. Available at: http://www.palmer.hs.columbia.edu/software/diffusion.html.
21. Palmer AG. r2r1_diffusion. Version 4.2, 2006. Accessed July 29, 2013. Available at: http://www.palmer.hs.columbia.edu/software/diffusion.html.
22. Mandel AM, Akke M, Palmer AG. Backbone dynamics of *Escherichia coli* ribonuclease HI: correlations with structure and function in an active enzyme. J Mol Biol 1995;246:144–163.
23. Cierpicki T, Bushweller JH. Charged gels as orienting media for measurement of residual dipolar couplings in soluble and integral membrane proteins. J Am Chem Soc 2004;126:16259–16266.
24. Ottiger M, Delaglio F, Bax A. Measurement of *J* and dipolar couplings from simplified two-dimensional NMR spectra. J Magn Reson 1998;131:373–378.

25. Sohn J, Parks J, Buhrman G. Experimental validation of the docking orientation of Cdc25 with its Cdk2-CycA protein substrate. Biochemistry 2005;44:16563–16573.
26. Sohn J, Buhrman G, Rudolph J. Kinetic and structural studies of specific protein-protein interactions in substrate catalysis by Cdc25B phosphatase. Biochemistry 2007;46:807–818.
27. Lipari G, Szabo A. Model-free approach to the interpretation of nuclear magnetic resonance relaxation in macromolecules. I. Theory and range of validity. J Am Chem Soc 1982;104:4546–4559.
28. Bax A. Weak alignment offers new NMR opportunities to study protein structure and dynamics. Protein Sci 2003;12:1–16.
29. Prestegard JH, al-Hashimi HM, Tolman JR. NMR structures of biomolecules using field oriented media and residual dipolar couplings. Q Rev Biophys 2000;33:371–424.
30. Shen Y, Delaglio F, Cornilescu G, Bax A. TALOS+: a hybrid method for predicting protein backbone torsion angles from NMR chemical shifts. J Biomol NMR 2009;44:213–223.